# Vascular Endothelial Cell Growth Factor Receptor 3–Mediated Activation of Lymphatic Endothelium Is Crucial for Tumor Cell Entry and Spread via Lymphatic Vessels

Yulong He,[1] Iiro Rajantie,[1] Katri Pajusola,[1] Michael Jeltsch,[1] Tanja Holopainen,[1] Seppo Yla-Herttuala,[2] Thomas Harding,[3] Karin Jooss,[3] Takashi Takahashi,[4] and Kari Alitalo[1]

[1]Molecular/Cancer Biology Laboratory and Ludwig Institute for Cancer Research, Biomedicum Helsinki and Helsinki University Central Hospital, University of Helsinki, Helsinki, Finland; [2]A.I. Virtanen Institute, University of Kuopio, Kuopio, Finland; [3]Cell Genesys, Inc., South San Francisco, California; and [4]Division of Molecular Carcinogenesis, Center for Neurological Disease and Cancer, Nagoya University Graduate School of Medicine, Nagoya, Japan

## Abstract

**Lymphangiogenic growth factors vascular endothelial growth factor (VEGF)-C and VEGF-D have been shown to promote lymphatic metastasis by inducing tumor-associated lymphangiogenesis. In this study, we have investigated how tumor cells gain access into lymphatic vessels and at what stage tumor cells initiate metastasis. We show that VEGF-C produced by tumor cells induced extensive lymphatic sprouting towards the tumor cells as well as dilation of the draining lymphatic vessels, suggesting an active role of lymphatic endothelial cells in lymphatic metastasis. A significant increase in lymphatic vessel growth occurred between 2 and 3 weeks after tumor xenotransplantation, and lymph node metastasis occurred at the same stage. These processes were blocked dose-dependently by inhibition of VEGF receptor 3 (VEGFR-3) signaling by systemic delivery of a soluble VEGFR-3-immunoglobulin (Ig) fusion protein via adenoviral or adeno-associated viral vectors. However, VEGFR-3-Ig did not suppress lymph node metastasis when the treatment was started at a later stage after the tumor cells had already spread out, suggesting that tumor cell entry into lymphatic vessels is a key step during tumor dissemination via the lymphatics. Whereas lymphangiogenesis and lymph node metastasis were significantly inhibited by VEGFR-3-Ig, some tumor cells were still detected in the lymph nodes in some of the treated mice. This indicates that complete blockade of lymphatic metastasis may require the targeting of both tumor lymphangiogenesis and tumor cell invasion.** (Cancer Res 2005; 65(11): 4739-46)

## Introduction

The dissemination of cancer cells to distant sites is known to occur via both lymphatic and blood vessels. During the last few years, there has been a dramatic increase in studies of the mechanisms of tumor-associated lymphangiogenesis and lymphatic metastasis. It has been recognized that lymphangiogenic growth factors promote cancer cell spread to regional lymph nodes (1–4). Two such factors have thus far been characterized, named vascular endothelial growth factor (VEGF)-C and VEGF-D. Both have been shown to induce lymphangiogenesis in several *in vivo* models (5–10). The essential role of VEGF receptor 3 (VEGFR-3) signaling in the development of the lymphatic system has recently been validated also by using genetic models (7, 11, 12).

A correlation between VEGF-C or VEGF-D expression and regional lymph node metastasis has been documented in a variety of human cancers (2, 3). Peripheral and/or intratumoral lymphatic vessels have been detected in some primary human cancers (13–16), in a variety of tumor xenografts overexpressing VEGF-C or VEGF-D (10, 17–20), and in chemically induced orthotopic squamous cell carcinomas in mice (21) as well as in a transgenic mouse tumor model (22). We have further shown that besides VEGF-C or VEGF-D, tumor lymphangiogenesis is also dependent on a preexisting network of lymphatic vessels but does not involve incorporation of bone marrow–derived progenitor cells (23). Inhibition of VEGFR-3 signaling has been shown to block tumor lymphangiogenesis (18) and lymph node metastasis (19, 24).

However, mechanisms of lymphatic tumor metastasis are still poorly understood. Here we have analyzed the interactions of LNM35 tumor cells, which express high levels of VEGF-C (19), with lymphatic endothelial cells by fluorescence microscopy using a stable enhanced green fluorescent protein (EGFP)–expressing tumor cell line (LNM35/EGFP) and immunostaining for a lymphatic endothelial marker. Tumor cells expressing firefly luciferase were also established and used to monitor tumor metastasis using a bioluminescence imaging system. Based on the data from our study, we propose that activation of lymphatic endothelial cells by VEGF-C produced by the tumor cells leads to lymphatic vessel destabilization, seen as vessel sprouting, leakage, and enlargement. This destabilization facilitates tumor cell entry into the lymphatic vessels. Also, tumor-induced increase in the diameter of the collecting lymphatic vessels was associated with enhanced passage of clusters of tumor cells to the sentinel lymph nodes. VEGFR-3-immunoglobulin (Ig) could block the lymphatic vessel destabilization, but it had no significant effect on the growth of the metastases once they had occurred.

## Materials and Methods

**Establishment of stable enhanced green fluorescent protein– and luciferase-expressing tumor cell lines.** The human lung cancer cell line NCI-H460-LNM35 (i.e., LNM35) was established and maintained as previously described (25). LNM35/EGFP and LNM35/Luciferase (LNM35/Luc) cells were established by infecting LNM35 cells with AAV-EGFP or AAV-Luc viruses, and $EGFP^+$ or $Luc^+$ clones were isolated by means of limiting dilution.

**Production of recombinant adeno-associated viruses (AAV-VEGFR-3-Ig).** The adeno-associated viral (AAV) vector psub-CAG-WPRE was cloned by substituting the cytomegalovirus (CMV) promoter fragment of psub-CMV-WPRE (26) with the CMV-chicken β-actin insert (27). The cDNA

**Requests for reprints:** Kari Alitalo, Molecular/Cancer Biology Laboratory and Ludwig Institute for Cancer Research, Biomedicum Helsinki and Helsinki University Central Hospital, University of Helsinki, P.O. Box 63 (Haartmaninkatu 8), 00014 Helsinki, Finland. Phone: 358-9191-25511; Fax: 358-9-912-25510; E-mail: kari.alitalo@helsinki.fi.

encoding the soluble VEGFR-3-Ig fusion protein (11) was cloned as a blunt-end fragment into the psub-CAG-WPRE plasmid, and the recombinant AAV viruses (AAV serotype 2) were produced as previously described (12). HeLa cells were used for expression analysis after transduction with AAV-VEGFR-3-Ig (multiplicity of infection: 2,000) according to the standard protocol.

***In vivo* delivery of VEGFR-3-Ig by adenoviral or adeno-associated viral vectors.** Recombinant adenoviruses expressing the VEGFR-3-Ig fusion protein (AdVEGFR-3-Ig; ref. 18) or β-galactosidase [AdLacZ; 1.0e+9 plaque-forming unit (pfu) per mouse; ref. 28] were administered via the tail vein 1 day after the tumor implantation. For the titration experiment, different doses of AdVEGFR-3-Ig (1.0e+9, 1.2e+8, 1.5e+7, or 2.0e+6 pfu) were used. Blood was collected from both the treated and control mice 1 week after the treatment, and the serum concentration of VEGFR-3-Ig was determined by ELISA, as previously described (11). In the ear tumor experiment, recombinant adenoviruses were administered via the tail vein 1 day before the tumor implantation.

For muscle injection with AAV viruses, mice were anesthetized with a mixture of Rompun (40 mg/kg mouse body weight, Bayer, Germany) and Ketalar (50 mg/kg, Pfizer, New York, NY). AAV-VEGFR-3-Ig (4.0e+11 viral genomes) was injected i.m. into both quadricep muscles ($2 \times 50$ μL), and AAV-EGFP was used as control. Blood from the treated and control mice was collected 3 weeks later and also at the time of sacrifice. Circulating VEGFR-3-Ig was determined as previously described (11).

**Xenotransplantation, excision, and analysis of tumors.** The Provincial State Office of Southern Finland approved all experiments, which were done in accordance with the institutional guidelines. Tumor implantation and treatment with either AdVEGFR-3-Ig or AdLacZ were done as described (19). Tumors were excised 1, 2, or 3 weeks after tumor implantation. Mice were allowed to recover and sacrificed within 7 weeks after the removal of primary tumors. Tissues were collected and processed for histology. Lymph nodes were measured and also weighed. In separate experiments, LNM35/EGFP cells ($1 \times 10^5$-$5 \times 10^5$ in 30 μL) were injected s.c. into the ears of the nude mice, and mice were treated as above ($n = 6$ for each group). Tumor-transplanted ears were analyzed within 2 weeks.

In experiments using AAV, tumors were implanted in SCID mice 3 weeks after the first administration of AAV-VEGFR-3-Ig. Mice were sacrificed within 5 weeks, and tumors, some internal organs including the lungs, and axillary lymph nodes were collected and analyzed under a dissecting LEICA MZFLIII microscope for EGFP signal. The lymph node volumes were calculated as described (29). Samples were processed as above for further histology.

In experiments with BrdUrd labeling, each mouse was injected i.p. with 0.5 mL of BrdUrd (5 mg/mL, Sigma, St. Louis, MO) to mark proliferating cells 1 hour before sacrifice. Tissues were collected and processed as above.

***In vivo* imaging of tumor metastasis and quantification of bioluminescence signal.** Ten minutes before *in vivo* imaging, mice were injected i.p. with D-luciferin (Synchem, Germany) at 150 mg/kg mouse body weight. Mice were then anesthetized as described above, and the light emitted from the bioluminescent tumors or metastatic lesions was detected using the IVIS Imaging System (Xenogen, Alameda, CA). Signal was digitized and electronically displayed as a pseudocolor overlay onto a gray scale animal image. Images and measurements of bioluminescent signals were acquired using the Living Image software (Xenogen). After imaging, the animals were euthanized, and organs of interest were removed, arranged on black, bioluminescence-free paper, and *ex vivo* imaged. A region of interest was manually selected over relevant regions of signal intensity. In this study, the area of the region of interest covered the whole axillary lymph nodes and was kept constant for all the samples. The region of interest was quantified as photons per second per square centimeter per steradian using the Living Image software. Background bioluminescence was measured for the same-sized region of interest without samples and subtracted.

**Immunofluorescence staining.** For whole-mount staining, tissues were fixed and stained as previously described (23). Samples were then mounted with Vectashield (Vector Laboratories, Burlingame, CA) and analyzed with a Zeiss LSM510 confocal microscope. For staining of tissue sections, paraffin sections (6 μm) of fixed tissue were immunostained with monoclonal antibodies against platelet/endothelial cell adhesion molecule 1 (PECAM-1; PharMingen, Franklin Lakes, NJ) and LYVE-1 as previously described (30, 31). The polyclonal antiserum against human LYVE-1 was produced in our laboratory. The extracellular domain of human LYVE-1 (residues 1-232, Uniprot Q9Y5Y7) was fused to the Fc part of human IgG1 and produced using the Bac-to-Bac system (Invitrogen, Netherlands). Immunization was started with 0.4 mg protein per rabbit in Freund's complete adjuvant. Booster injections containing Freund's incomplete adjuvant and 0.2 mg protein per rabbit were given after 3, 6, 9, and 12 weeks, followed by terminal bleeding 1 week after the last booster injection. In some experiments, proliferating cells in the sections were first stained by using the proliferating cell nuclear antigen or BrdUrd staining kit (Zymed, San Francisco, CA) and then stained for LYVE-1.

**Fluorescent microlymphography.** The functional lymphatic network surrounding the tumors s.c. implanted in the ears was visualized by fluorescent microlymphography using dextran conjugated with FITC (molecular weight: 2,000 kDa, Sigma), which was injected intradermally into the ears. The lymphatic vessels were then examined using the dissection microscope.

**Statistical analysis.** Statistical analysis was done with unpaired *t* test. All statistical tests were two sided.

## Results

**Lymphatic vessel sprouting and dilation facilitates tumor cell entry and spread to regional lymph nodes.** To gain insight into how tumor cells get access into lymphatic vessels, fluorescently labeled LNM35 tumor cells were implanted in the s.c. tissue of mouse ear and analyzed after various time points. Whole-mount staining for LYVE-1 revealed extensive lymphatic vessel sprouting towards the EGFP-expressing tumor cells (Fig. 1*A*, day 4; and Fig. 1*B*, day 12; arrowheads point to lymphatic sprouts). Lymphatic vessels often grew around single tumor cells or tumor cell masses, enveloping the tumor cells (Fig. 1*B*). Similar elongated lymphatic endothelial cells were observed around clusters of tumor cells when these cells were cocultured *in vitro* (data not shown). In mice treated with AdVEGFR-3-Ig, the lymphatic sprouting was inhibited, but the tumor cells could still co-opt pre-existing lymphatic vessels (Fig. 1*C* and *D*). The treatment inhibited tumor-associated lymphatic vessel growth and dye leakage from the newly formed vessels as seen in microlymphangiography of the s.c. implanted tumor areas (compare Fig. 1*E* and *F*).

To visualize the spread of tumor cells via the lymphatic vessels, mice bearing s.c. LNM35/EGFP tumors were anesthetized; a skin flap containing the collecting lymphatic vessels draining the tumor was inverted and analyzed by fluorescence microscopy at week 5 after tumor implantation. The draining lymphatic vessels were clearly dilated (Fig. 2*A* and *B*, *arrowheads*) when compared with the collecting lymphatic vessels in the treated mice (Fig. 2*C*) and in the skin of a mouse without tumor visualized using FITC-dextran microlymphography (Fig. 2*D*). Furthermore, both single tumor cells and tumor cell masses were observed in the lymphatic vessels of the untreated mice (Fig. 2*A* and *B*, *arrows*), but not in the AdVEGFR-3-Ig–treated tumor-bearing mice (Fig. 2*C*). As an example, Fig. 2*B* shows a high-magnification view of a collecting lymphatic vessel from an untreated tumor-bearing mouse, where typical groups of $EGFP^+$ tumor cells can be seen.

To assess if the dilation of the collecting lymphatic vessels was accompanied by lymphatic endothelial cell proliferation, a bolus of BrdUrd was administered 1 hour before the mice were sacrificed. About 8% of the lymphatic endothelial cells were proliferating in the peritumoral draining lymphatic vessels of the control mice as seen by double-labeling for LYVE-1 (*red*) and nuclear BrdUrd (*brown*; Fig. 2*E*). However, proliferating lymphatic endothelial cells were only rarely observed in the AdVEGFR-3-Ig–treated mice (Fig. 2*F*).

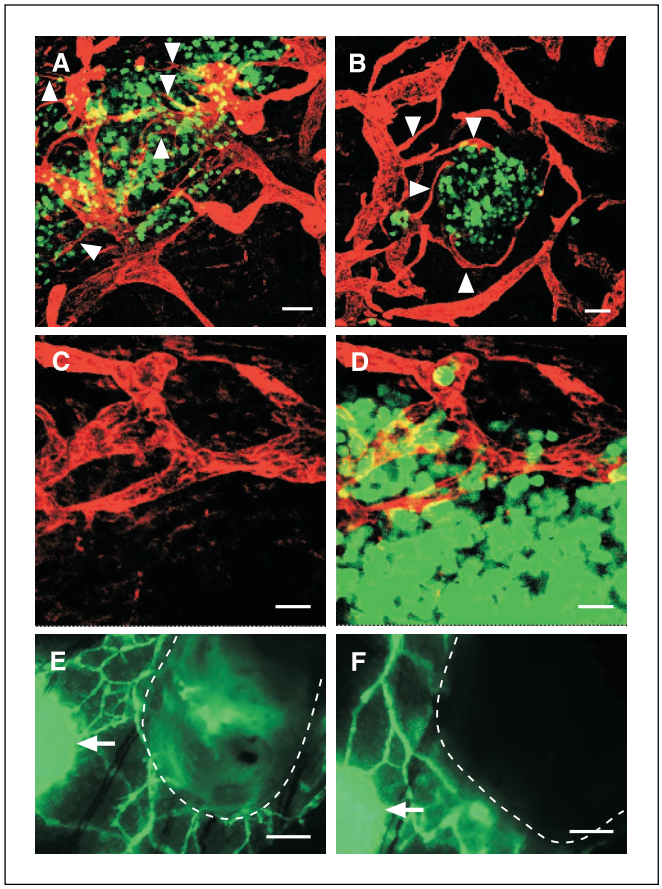


**Figure 1.** Whole-mount analysis of tumor induced lymphatic sprouting by confocal microscopy. *A* and *B,* whole-mount staining for LYVE-1 of ears implanted with EGFP-expressing tumor cells. Note extensive lymphatic sprouting (*A*, *arrowheads*; day 4), and lymphatic vessels growing around a tumor cell mass (*B*; day 12). *C* and *D,* tumor induction of lymphatic sprouting was inhibited in mice treated with AdVEGFR-3-Ig (*C,* lymphatics alone; *D,* overlay of lymphatics with tumor cells). *E* and *F,* FITC-dextran microlymphography of the lymphatic vessels surrounding tumors implanted in the s.c. tissues of ears from mice treated with AdLacZ (*E*) or AdVEGFR-3-Ig (*F*). *Dotted lines,* tumor position; *arrows,* FITC-dextran injection sites. Bar: 100 μm (*A*), 80 μm (*B*), 40 μm (*C* and *D*), and 800 μm (*E* and *F*).

**Dose-dependent inhibition of macrometastasis by VEGFR-3-Ig delivered via adenoviral vectors.** To investigate the effect of different levels of circulating VEGFR-3-Ig on lymphatic metastasis, SCID mice bearing luciferase-expressing LNM35 tumors were injected with different doses of AdVEGFR-3-Ig via the tail vein. Serum concentrations of the VEGFR-3-Ig fusion protein determined 1 week after the injection correlated with the adenovirus dose, as shown in Fig. 3*A*. Bioluminescent signals emitted from the lymph nodes of the treated and control mice were quantified as photons per second per square centimeter per steradian 5 weeks after tumor implantation (Fig. 3*B*). As evident from the figure, some suppression of lymph node metastasis was obtained even with the lowest dose of 2.0e+6 pfu of AdVEGFR-3-Ig.

A dramatic increase in lymph node size (macrometastasis) occurred in all mice in the control group (6 of 6), and also in some of the mice receiving AdVEGFR-3-Ig (1 of 6 mice with 1.5e+7 pfu; 2 of 6 mice with 2.0e+6 pfu). However, although macrometastasis was rare in tumor-bearing mice receiving high doses of AdVEGFR-3-Ig (1.0e+9 pfu), micrometastasis as determined by the presence of the luciferase signal in the lymph nodes still occurred in most of the treated mice. The lymph node shown in Fig. 3*C* does not have metastasis; typical signals from micrometastases are seen in Fig. 3*D* to *F*. Four of six mice in the 1.0e+9 pfu group, six of six mice in the 1.2e+8 pfu group, five of six mice in the 1.5e+7 pfu group, and five of five mice in the 2.0e+6 pfu group had micrometastasis.

When the tumor was removed 2 weeks after implantation, only one of five of the untreated SCID mice developed macrometastasis by week 6 (Fig. 3*G*, *lane AdLacZ/W2*). However, when the tumor was removed 3 weeks after implantation, five of six of the untreated mice developed macrometastasis (Fig. 3*G*, *lane AdLacZ/W3*). Consistent with our previous results (19), no macrometastases were observed in the AdVEGFR-3-Ig (1.0e+9 pfu)–treated mice. Even more importantly, no micrometastases were observed in any of the AdVEGFR-3-Ig–treated mice when the tumor was removed at week 2 or 3 (Fig. 3*G*, *lanes AdR3-Ig*).

**Long-term VEGFR-3-Ig expression via adeno-associated viral vectors inhibits lymph node macrometastasis but not micrometastasis.** Inhibition of lymphatic metastasis was also achieved in tumor-bearing mice treated with the AAV-VEGFR-3-Ig. In nude mice receiving AAV-VEGFR-3-Ig (1.0e+11 viral genomes) by i.m. delivery, the serum concentration of VEGFR-3-Ig at week 3 was 393.4 ± 185.2 ng/mL ($n$ = 10). There was only a slight decrease of the circulating VEGFR-3-Ig 9 weeks after the administration of the

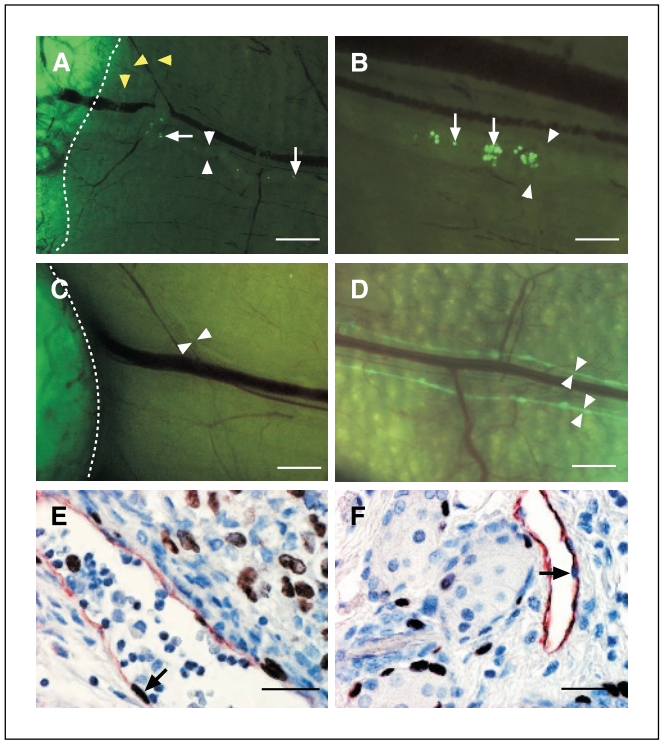


**Figure 2.** Invasion of tumor cells into lymphatic vessels. *A,* a dilated collecting lymphatic vessel (*white arrowheads*) with invading tumor cells (EGFP$^+$, *arrows*). *B,* high magnification showing the EGFP$^+$ cells and cell clusters in the collecting lymphatic vessel. *C,* dilation of the collecting lymphatic vessel induced by the tumor was inhibited by blocking VEGFR-3 signaling using AdVEGFR-3-Ig. *D,* visualization of the collecting lymphatic vessels in the skin of a mouse without tumors by FITC-dextran microlymphography. *A* and *C, dotted lines,* tumor position. *Yellow arrowheads*, small collecting lymphatic vessels connecting to a large draining lymphatic vessel (*A*). *White arrowheads,* position of the draining lymphatic vessel (*A-D*). *E* and *F,* double staining of LYVE-1 and BrdUrd in tumor sections (*E,* AdLacZ; *F,* AdVEGFR-3-Ig). *Arrows,* lymphatic endothelial cells of peritumoral draining lymphatic vessels positive (*E*) and negative (*F*) for BrdUrd. Bar: 800 μm (*A*, *C*, and *D*), 200 μm (*B*), and 50 μm (*E* and *F*).

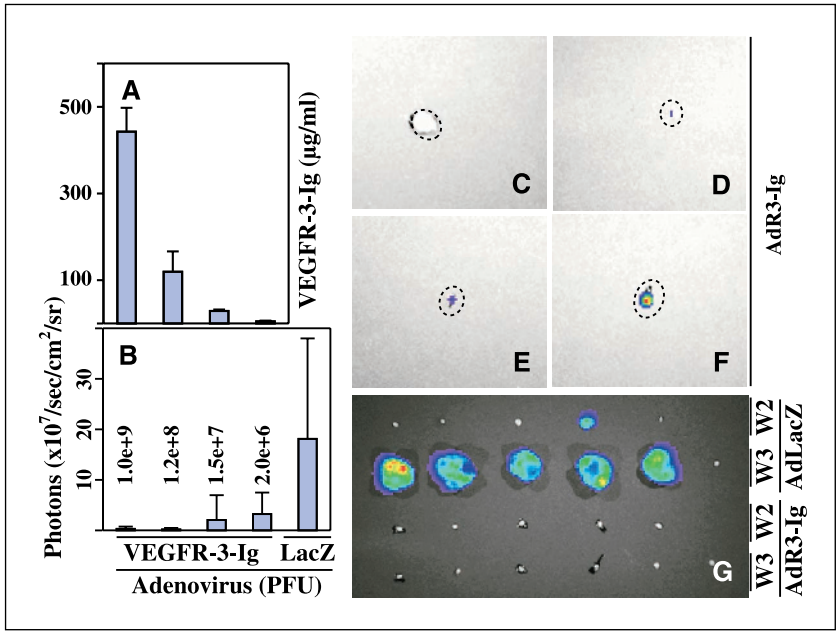


**Figure 3.** *Ex vivo* imaging of lymph nodes with tumor metastasis using a bioluminescence imaging system. *A,* plotting of the serum concentration of VEGFR-3-Ig in mice receiving different doses of AdVEGFR-3-Ig (1.0e+9 pfu: 442.54 ± 55.21 μg/mL, $n$ = 11; 1.2e+8 pfu: 119.27 ± 46.89 μg/mL, $n$ = 7; 1.5e+7 pfu: 28.83 ± 3.17 μg/mL, $n$ = 6; and 2.0e+6 pfu: 4.67 ± 1.77 μg/mL, $n$ = 5). *B,* bioluminescent signals emitted from the lymph nodes of mice treated with different doses of AdVEGFR-3-Ig or AdLacZ (1.0e+9 pfu) were quantified as photons per second per square centimeter per steradian [× $10^7$, mean ± SD; 0.30 ± 0.46 ($n$ = 6), 0.18 ± 0.29 ($n$ = 6), 2.05 ± 4.90 ($n$ = 6), 3.21 ± 4.26 ($n$ = 5), and 18.10 ± 19.90 ($n$ = 6), respectively]. *C-F,* representative images of axillary lymph nodes (*dotted circles*) from the mice treated with AdVEGFR-3-Ig (1.0e+9 pfu). Note that micrometastasis to axillary lymph nodes as determined by the presence of bioluminescent signals occurred also in some of the treated mice (*D-F*). *G,* images of axillary lymph nodes from tumor-bearing mice receiving AdLacZ and AdR3-Ig (*W2* and *W3,* primary tumors removed at week 2 or 3). Tumor metastasis to lymph nodes was not observed in the mice treated with AdR3-Ig when the primary tumors were surgically removed within 3 weeks.

recombinant AAV virus (333.4 ± 151.2 ng/mL, $n$ = 9). This indicates that stable and long-term expression of VEGFR-3-Ig was achieved by AAV-mediated gene delivery. SCID mice that were injected i.m. with AAV-VEGFR-3-Ig (4.0e+11 viral genomes) had 2.02 ± 0.58 μg/mL ($n$ = 12) of VEGFR-3-Ig in the circulation 3 weeks after virus administration. There was a significant difference in lymph node volume between the treated and untreated mice 5 weeks after tumor inoculation. In the AAV-VEGFR-3-Ig group, the lymph node volume was 2.51 ± 1.61 $mm^3$ ($n$ = 12), whereas it was 13.10 ± 14.59 $mm^3$ in the untreated group ($n$ = 6, $P$ = 0.0209, unpaired $t$ test; Fig. 4*A*). In the mice treated with AAV-VEGFR-3-Ig, macroscopically evident metastasis, which was present in the untreated group receiving AAV-EGFP (2 of 6; the rest contained micrometastasis), was not observed.

Shown in the top row of Fig. 4 (*B-E*) are representative axillary lymph nodes from tumor-bearing mice in the treated group, and in the *bottom* row (*F-I*) are lymph nodes from the untreated group. Note that these figures are not shown with the same magnification to better visualize the $EGFP^+$ micrometastases in the top row. Note also that in Fig. 4*H* and *I*, the upper lymph node from the tumor side was enlarged and densely invaded by the $EGFP^+$ tumor cells as compared with the typical lymph node from the contralateral side below. As with the mice receiving AdVEGFR-3-Ig, most of the lymph nodes from the mice receiving AAV-VEGFR-3-Ig (9 of 12) contained $EGFP^+$ tumor cells, suggesting that micrometastasis occurred in the treated mice as well (Fig. 4*B-E*, *arrows*).

**Tumor lymphangiogenesis occurs later than angiogenesis.** To investigate when lymphangiogenesis occurs during tumor growth, the tumors were excised at 1, 2, or 3 weeks after xenotransplantation into nude mice. The lymphatic vessels in the tumors were analyzed by immunostaining using antibodies against the lymphatic endothelial marker LYVE-1. No lymphatic vessels were seen in the tumors or peritumoral areas at week 1 (Fig. 5*A*, *B*, and *G*), whereas some were detected in week 2 tumors (Fig. 5*G*). However, there was a dramatic increase of lymphatic vessels in week 3 tumors and peritumoral tissues (Fig. 5*C*, *D*, and *G*). The average number of intratumoral LYVE-1–positive vessels determined from three microscopic fields of the highest vessel density is shown in Fig. 5*G* (week 2 tumor, mean ± SD: 2.07 ± 3.22 vessels/grid, $n$ = 6; week 3 tumor: 12.17 ± 2.63, $n$ = 6). There was a significant increase in the lymphatic vessel density between weeks 2 and 3 as determined by unpaired $t$ test (two-tailed $P$ = 0.0001). Intratumoral lymphatic vessels were not observed in tumors from AdVEGFR-3-Ig–treated mice at week 1 or 2, and only few were detected at week 3 (0.37 ± 0.64, mean ± SD, $n$ = 10; Fig. 5*G*).

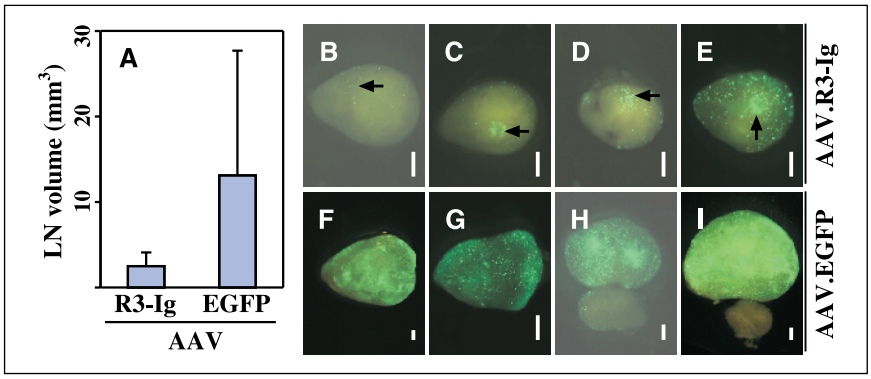


**Figure 4.** Analysis of tumor metastasis in axillary lymph nodes by fluorescence microscopy. *A,* plotting of the lymph node volumes (in cubic millimeters) from AAV-EGFP– and AAV-VEGFR-3-Ig–treated mice, calculated as follows: volume = (π / 6) × (length × width)$^{3/2}$. *B-E,* representative lymph nodes from mice bearing the LNM35/EGFP tumors treated with AAV-VEGFR-3-Ig (4.0e+11 viral genomes). Note that the lymph nodes also contain some $EGFP^+$ tumor cells (micrometastasis; *arrows*). *F-I,* representative lymph nodes from mice treated with AAV-EGFP. Lymph nodes from the control group were significantly enlarged on the tumor side (*H* and *I*, *top*) in comparison with those (*H* and *I*, *bottom*) from the side without tumor. Bar, 500 μm (*B-I*).

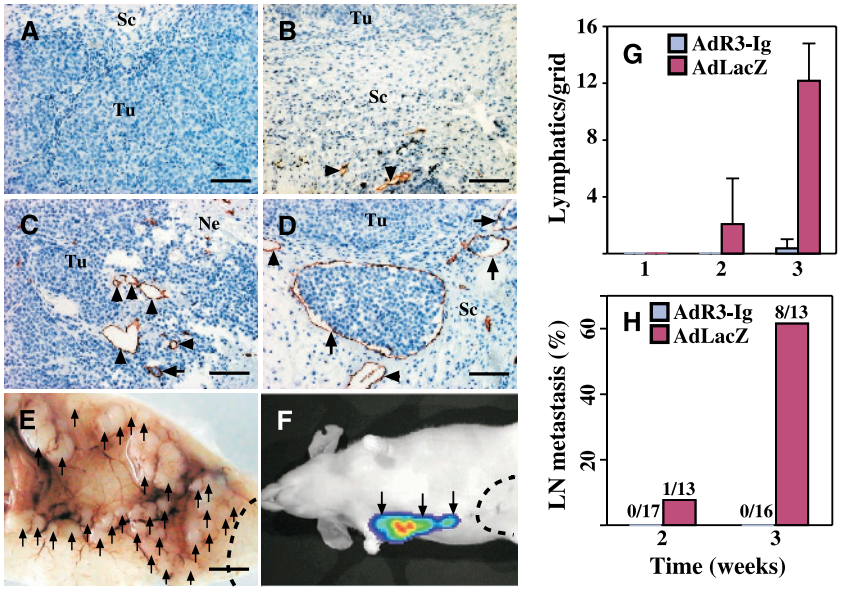


**Figure 5.** Lymphangiogenesis in the LNM35 tumors excised at different stages of tumor growth. Immunohistochemical staining for LYVE-1 to identify the lymphatic vessels (*A-D*). *A* and *B,* sections of the week 1 tumors; *C* and *D,* sections of the week 3 tumors. *Tu,* tumor; *Sc,* s.c. tissues; *Ne,* necrotic regions. *E,* metastatic foci were established along the collecting lymphatic vessels in the skin of SCID mice. *Arrows,* metastatic tumor nodules; *dotted line,* primary tumor position. *F,* imaging of tumor metastasis in the axillary lymph nodes and the collecting lymphatic vessels (*arrows*) of a nude mouse by the bioluminescence imaging system. *Dotted line,* position of a primary tumor excised at week 3. Bar: 100 μm (*A-D*) and 3.5 mm (*E*). *G,* quantification of LYVE-1–stained vessels in three microscopic fields of the highest vessel density. There is a significant increase of LYVE-1–stained vessels ($P$ = 0.0001, unpaired $t$ test) in week 3 tumors compared with those of week 2 tumors. *H,* percentage of mice with lymph node metastasis in the AdVEGFR-3-Ig–treated and control mice when tumors were excised at week 2 and 3 stages.

Staining of tumor sections for PECAM-1, a panendothelial marker, showed robust angiogenesis at all stages of tumor growth, and in both intratumoral and peritumoral tissues. The intratumoral vessel density, as determined from three microscopic fields of the highest vessel density, was 43.08 ± 7.41 ($n$ = 4), 30.14 ± 7.05 ($n$ = 5), and 31.04 ± 5.05 vessels/grid ($n$ = 5) in week 1, 2, and 3 tumors from the control mice, and 39.28 ± 10.53 ($n$ = 4), 28.40 ± 6.53 ($n$ = 6), and 26.63 ± 7.05 vessels/grid ($n$ = 6), respectively, in mice treated with AdVEGFR-3-Ig. Thus, there was no significant difference in the blood vessel density between tumors from the AdVEGFR-3-Ig–treated and control mice at these time points, although the treated tumors were slightly smaller.[5] We are currently investigating in more detail the effect of various VEGFR-3 inhibitors on tumor growth.

**Initiation of lymphatic metastasis correlates with tumor lymphangiogenesis.** To determine when tumor cells start to spread to regional lymph nodes, the tumors were excised at different stages of growth in nude mice as described above, the mice were allowed to recover and analyzed 8 weeks after the initial xenotransplantation. In the control group, no lymph node metastasis was detected when the tumors were excised at week 1. Lymph node metastasis was also rarely detected when tumors were excised at week 2 (1 of 13; Fig. 5*H*). However, about two thirds of the mice developed lymph node metastasis after tumors were removed at week 3 (8 of 13; Fig. 5*H*). Therefore, similar to the SCID mice (Fig. 3*G*), tumor cell spread to regional lymph nodes was initiated primarily between weeks 2 and 3 after the xenotransplantation into nude mice. Consistent with the previous observations (19), no lymph node metastasis was detected in the AdVEGFR-3-Ig–treated mice by histologic analysis (Fig. 5*H*). Interestingly, tumor cells could proliferate in lymphatic vessels (Fig. 5*D*) and they established metastatic foci in the draining lymphatic vessels of both SCID mice and nude mice (Fig. 5*E* and *F*, respectively).

[5] Unpublished data.

**Blocking VEGFR-3 signaling does not suppress metastatic tumor growth in the lymph nodes.** In bioluminescence *in vivo* imaging using the IVIS Imaging system, pseudocolor images represent the spatial distribution of photon counts within the animal (blue, least intense; red, most intense). Pseudocolor images overlaid on the gray-scale reference image allow the monitoring of tumor progression and anatomic localization of tumor metastasis in the whole animal. Shown in Fig. 6 are representative images from the mice before (*A* and *D*) and after removal of the primary tumors at week 3 (*B*, *C*, *E*, and *F*). Lymph node metastasis was detected in the control mice (Fig. 6*D-F*, *arrows*), but not in the mice treated with AdVEGFR-3-Ig when analyzed 3 weeks after the removal of primary tumors (Fig. 6*B*). This is also shown in Fig. 6*G*, where axillary lymph nodes from the treated mice (*top row*) and control (*bottom row*) were analyzed by bioluminescent imaging *ex vivo*. Most mice in the control group developed lymph node metastasis (6 of 7; Fig. 6*G*, *bottom row*). Of note is that the only mouse with lymph node metastasis in the treated group (Fig. 6*G*, *top row*) had a very low concentration of serum VEGFR-3-Ig (data not shown). However, excision of the primary tumor on day 21, followed by administration of AdVEGFR-3-Ig starting on day 25, did not have a major effect on metastatic tumor growth in the lymph nodes (Fig. 6*C* and *H*). Furthermore, consistent with the observation of intralymphatic $EGFP^+$ tumor cell clusters, metastatic tumor cells could also be detected in the draining lymphatic vessels by using the bioluminescence imaging system (Fig. 6*E*, *arrowhead*).

## Discussion

This study shows that the lymphatic vessels undergo dramatic lymphangiogenic changes in response to nearby LNM35 tumor cells, including lymphatic endothelial cell sprouting and dilation of the lymphatic capillaries as well as dilation of the larger collecting lymphatic vessels draining the tumor area. Close interactions between the tumor cells and lymphatic endothelial cells suggest

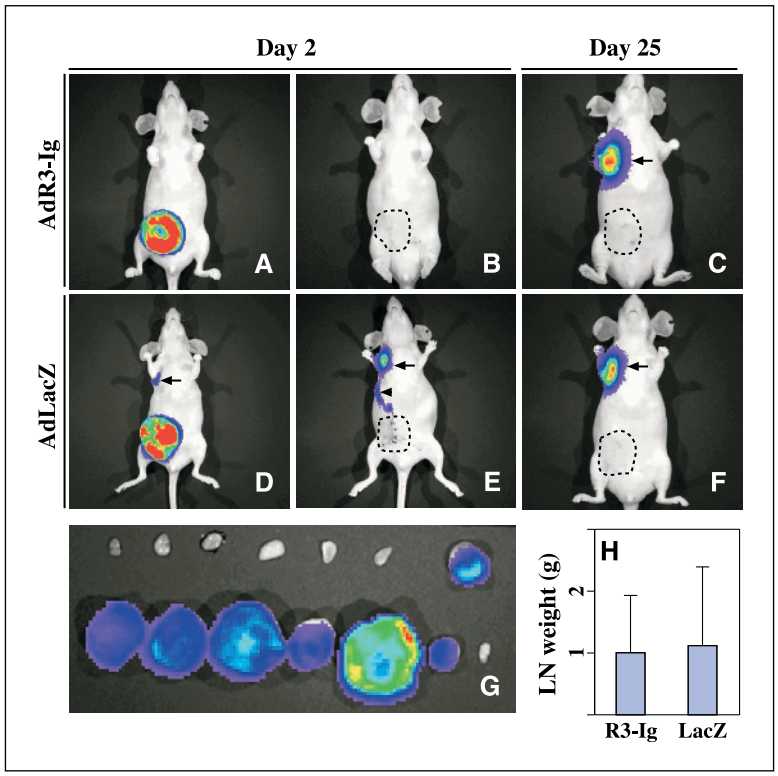


**Figure 6.** *In vivo* bioluminescence imaging of primary tumors and tumor metastasis. Representative images from the mice before (*A* and *D*) or after the removal of primary tumors at week 3 (*B*, *C*, *E*, and *F*). *A* and *B,* mice treated with AdVEGFR-3-Ig 1 day after tumor implantation (day 2). *C,* mice treated with AdVEGFR-3-Ig on day 25 showed metastasis in the axillary lymph nodes. *D-F,* images of tumor bearing mice receiving AdLacZ viruses. *Arrows,* tumor metastasis in the lymph nodes (*C-F*); *arrowheads,* metastatic tumor cells in the draining lymphatic vessel (*E*). *Dotted circles,* primary tumor positions. *G,* images of axillary lymph nodes from tumor-bearing mice treated with AdVEGFR-3-Ig (*top row*) or AdLacZ (*bottom row*). *H,* plotting of lymph node weight from the mice with lymph node metastasis treated with AdVEGFR-3-Ig (*R3-Ig*) or AdLacZ (*LacZ*) starting on day 25. Note that blocking VEGFR-3 signaling did not suppress the growth of metastatic tumor in the lymph nodes (R3-Ig: 1.0 ± 0.93 g, $n$ = 8; LacZ: 1.12 ± 1.27 g, $n$ = 5; $P$ = 0.8471).

that the lymphatic endothelial cells have an active role in tumor cell entry and spread via lymphatic vessels. Tumor lymphangiogenesis involving lymphatic sprouting and vessel dilation may in fact be a rate-limiting step during lymphatic tumor metastasis as blocking these processes by inhibition of VEGFR-3 signaling with the soluble VEGFR-3-Ig fusion protein delivered by adenoviral or AAV vectors significantly suppressed tumor metastasis to the lymph nodes. In contrast, tumor metastasis was not suppressed when the treatment was started 3 weeks after the tumor implantation, at a stage when the metastatic spreading had already occurred in most of the mice. This latter result indicates that the growth of the metastases in the lymph nodes was not significantly affected by the VEGFR-3-Ig fusion protein. Thus, inhibition of tumor cell entry into the lymphatic vessels seems critical for the suppression of lymph node metastasis.

Confocal analysis of whole-mount stained tumor-bearing ears revealed extensive lymphatic sprouting towards the tumor cells. In several cases, lymphatic vessel growth occurred around the tumors. It may be that the enveloping of the tumor cells or cell clusters by the lymphatic endothelial cells contributes to the lymphatic entry and metastasis. Some studies have suggested that also hematogenous metastases are often coated with blood vascular endothelial cells (32). It is also likely that destabilization of the lymphatic vessel wall induced by tumor-secreted VEGF-C facilitates tumor cell invasion into the lymphatics. This is supported by the leakage of high molecular weight FITC-dextran from newly generated lymphatic vessels to the interstitium on VEGF-C induced lymphangiogenesis,[6] suggesting some loss of the integrity of the valve-like junctions between the lymphatic endothelial cells. Furthermore, lymphatic vessel dilation may increase its capacity to support tumor cell transit as single cells or cell clumps. Although lymphatic endothelial cell proliferation was detected by BrdUrd labeling in the peritumoral lymphatic vessels, lymphatic endothelial cell shape changes upon lymphangiogenic growth factor stimulation may also contribute to the vessel dilation. Finally, tumor-induced lymphatic sprouting and dilation of the collecting lymphatic vessels could be inhibited by VEGFR-3-Ig delivered via the adenoviral vector, indicating that VEGFR-3 signaling is essential in these processes.

Even in the presence of inhibitory levels of VEGFR-3-Ig, micrometastasis of individual EGFP-positive cells or small tumor cell clusters, as well as bioluminescent signals originating from few luciferase-expressing tumor cells in the lymph nodes, was observed in the SCID mice. However, micrometastasis was rarely observed in mice treated with AdVEGFR-3-Ig if the primary tumor was removed at or before week 3. It is possible that the occurrence of micrometastasis was a late event due to a decrease of circulating VEGFR-3-Ig in mice treated with the adenoviral vector (19). However, its occurrence despite long-term inhibition with AAV-VEGFR-3-Ig suggests that micrometastasis may also reflect a low rate of tumor cell invasion and metastasis without the need for lymphatic endothelial cell activation.

Although the LNM35 tumor cells have been reported to be capable of spontaneous metastasis to the regional lymph nodes when s.c. implanted (19, 25), it has not been clear when the tumor cells initiate dissemination. In this study, the primary tumors were excised at different stages to determine the stages at which tumor lymphangiogenesis and metastasis occur. Lymphatics were first detected in some of the week 2 tumors, and a dramatic increase was observed in week 3 tumors both intratumorally and peritumorally. Such late occurrence of lymphangiogenesis in comparison with angiogenesis has also been reported in wound-healing studies (33). The delay observed

[6] Our present data and unpublished observations using VEGF-C expression.

was not due to a slow onset of VEGF-C expression as immunostaining did not show obvious differences in the amount of VEGF-C in week 1, 2, or 3 tumors.[7] The finding of intratumoral lymphatic vessels mainly in the interstitial spaces between the expanding tumor cell masses or around necrotic areas suggests that factors such as mechanical stress, owing to the rapid expansion of the tumor, restrain lymphatic growth. Furthermore, the availability of the pre-existing lymphatic vessels may be another rate-limiting factor, depending on the anatomic location. In our previous study, tumors were shown to co-opt a pre-existing lymphatic network, from which new lymphatic vessels originated with little, if any, incorporation of bone marrow–derived endothelial progenitor cells (23). It is therefore likely that tumor lymphangiogenesis lags behind angiogenesis due to lack of lymphatic vessels surrounding the tumor at early stages.

The time of onset of lymph node metastasis roughly coincided with the maximal tumor lymphangiogenesis, further validating the essential role of the tumor induced lymphangiogenic process in lymphatic metastasis. We also observed that metastatic foci were formed along the collecting lymphatic vessels draining into the ipsilateral lymph nodes, but not on the contralateral side. At this point, we cannot be sure if these metastases originated from individual cells or cell aggregates. It is likely that the tumor cells spreading as emboli get arrested in the draining lymphatic vessel before they reach the lymph node; they subsequently can establish metastatic foci within lymphatic vessels without the need for extravasation. Similar observations have been made in the 293-VEGF-D tumor model (10). A comparable phenomenon called *lymphangiosis carcinomatosa* has been found to be an independent predictor of lymph node metastasis in patients with mammary cancer (34). Furthermore, only one third of nude mice developed lung metastases when the primary tumors were removed at week 3, although macroscopically evident lymph node metastases were present in about two thirds of the mice. This suggests that in this model, lymphatic tumor spread contributes little, if any, to systemic metastasis at the early stages. Thus, LNM35 tumor cells apparently survive in the blood circulation and colonize the lung via this route. It could be that the lymph nodes actually act as barriers for tumor cell dissemination in some tumor models, but as bridgeheads in others (24).

In summary, the results of this study provide evidence suggesting that activation of lymphatic endothelium by tumor-secreted VEGF-C promotes lymphatic metastasis by facilitating tumor cell entry and transit in the lymphatic vessels. The process seems to include VEGF-C induced lymphatic sprouting from the pre-existing lymphatic network, lymphatic endothelial enveloping of single tumor cells or tumor emboli, as well as dilation of collecting lymphatic vessels, presumably facilitating further spread. Furthermore, tumor cells can establish metastatic foci within lymphatic vessels without extravasation, particularly in severely immunocompromised mice. Finally, the blocking of VEGFR-3 signaling can inhibit the entry of tumor cells into the lymphatic vessels and decrease their transit to the lymph nodes, but is ineffective thereafter. The findings of our study provide insights into the mechanisms underlying lymphatic tumor metastasis, and suggest that targeting lymphatic endothelial cells provides a potential therapeutic strategy for blocking metastasis.

[7] Our unpublished data.

## Acknowledgments

Received 12/22/2004; revised 2/23/2005; accepted 3/22/2005.

**Grant support:** Finnish Academy of Sciences, Biocentrum Helsinki, Human Frontier Science Program (HFSP R6P0231/2001-M), the Sigrid Juselius Foundation, the European Union (QLC1-CT-2001-01172 and QLK3-CT-2002-02059), and NIH (HD37243).

The costs of publication of this article were defrayed in part by the payment of page charges. This article must therefore be hereby marked *advertisement* in accordance with 18 U.S.C. Section 1734 solely to indicate this fact.

We kindly thank Paula Hyvarinen, Sanna Karttunen, Mari Helantera, and Tapio Tainola for excellent technical assistance.

## References

1. Stacker SA, Baldwin ME, Achen MG. The role of tumor lymphangiogenesis in metastatic spread. FASEB J 2002; 16:922–34.
2. He Y, Karpanen T, Alitalo K. Role of lymphangiogenic factors in tumor metastasis. Biochim Biophys Acta 2004;1654:3–12.
3. Stacker SA, Achen MG, Jussila L, Baldwin ME, Alitalo K. Metastasis: Lymphangiogenesis and cancer metastasis. Nat Rev Cancer 2002;2:573–83.
4. Oliver G, Detmar M. The rediscovery of the lymphatic system: old and new insights into the development and biological function of the lymphatic vasculature. Genes Dev 2002;16:773–83.
5. Jeltsch M, Kaipainen A, Joukov V, et al. Hyperplasia of lymphatic vessels in VEGF-C transgenic mice. Science 1997;276:1423–5.
6. Oh SJ, Jeltsch MM, Birkenhager R, et al. VEGF and VEGF-C: specific induction of angiogenesis and lymphangiogenesis in the differentiated avian chorioallantoic membrane. Dev Biol 1997;188:96–109.
7. Veikkola T, Jussila L, Makinen T, et al. Signalling via vascular endothelial growth factor receptor-3 is sufficient for lymphangiogenesis in transgenic mice. EMBO J 2001;20:1223–31.
8. Enholm B, Karpanen T, Jeltsch M, et al. Adenoviral expression of vascular endothelial growth factor-C induces lymphangiogenesis in the skin. Circ Res 2001; 88:623–9.
9. Saaristo A, Veikkola T, Tammela T, et al. Lymphangiogenic gene therapy with minimal blood vascular side effects. J Exp Med 2002;196:719–30.
10. Stacker SA, Caesar C, Baldwin ME, et al. VEGF-D promotes the metastatic spread of tumor cells via the lymphatics. Nat Med 2001;7:186–91.
11. Makinen T, Jussila L, Veikkola T, et al. Inhibition of lymphangiogenesis with resulting lymphedema in transgenic mice expressing soluble VEGF receptor-3. Nat Med 2001;7:199–205.
12. Karkkainen MJ, Saaristo A, Jussila L, et al. A model for gene therapy of human hereditary lymphedema. Proc Natl Acad Sci U S A 2001;98:12677–82.
13. Straume O, Jackson DG, Akslen LA. Independent prognostic impact of lymphatic vessel density and presence of low-grade lymphangiogenesis in cutaneous melanoma. Clin Cancer Res 2003;9:250–6.
14. Beasley NJ, Prevo R, Banerji S, et al. Intratumoral lymphangiogenesis and lymph node metastasis in head and neck cancer. Cancer Res 2002;62:1315–20.
15. Rubbia-Brandt L, Terris B, Giostra E, Dousset B, Morel P, Pepper MS. Lymphatic vessel density and vascular endothelial growth factor-C expression correlate with malignant behavior in human pancreatic endocrine tumors. Clin Cancer Res 2004;10: 6919–28.
16. Sipos B, Klapper W, Kruse ML, Kalthoff H, Kerjaschki D, Kloppel G. Expression of lymphangiogenic factors and evidence of intratumoral lymphangiogenesis in pancreatic endocrine tumors. Am J Pathol 2004;165: 1187–97.
17. Skobe M, Hawighorst T, Jackson DG, et al. Induction of tumor lymphangiogenesis by VEGF-C promotes breast cancer metastasis. Nat Med 2001;7:192–8.
18. Karpanen T, Egeblad M, Karkkainen MJ, et al. Vascular endothelial growth factor C promotes tumor lymphangiogenesis and intralymphatic tumor growth. Cancer Res 2001;61:1786–90.
19. He Y, Kozaki K, Karpanen T, et al. Suppression of tumor lymphangiogenesis and lymph node metastasis by blocking vascular endothelial growth factor receptor 3 signaling. J Natl Cancer Inst 2002;94:819–25.
20. Mattila MM, Ruohola JK, Karpanen T, Jackson DG, Alitalo K, Harkonen PL. VEGF-C induced lymphangiogenesis is associated with lymph node metastasis in orthotopic MCF-7 tumors. Int J Cancer 2002;98:946–51.
21. Hawighorst T, Oura H, Streit M, et al. Thrombospondin-1 selectively inhibits early-stage carcinogenesis and angiogenesis but not tumor lymphangiogenesis and lymphatic metastasis in transgenic mice. Oncogene 2002; 21:7945–56.
22. Mandriota SJ, Jussila L, Jeltsch M, et al. Vascular endothelial growth factor-C-mediated lymphangiogenesis promotes tumour metastasis. EMBO J 2001;20:672–82.

23. He Y, Rajantie I, Ilmonen M, et al. Preexisting lymphatic endothelium but not endothelial progenitor cells are essential for tumor lymphangiogenesis and lymphatic metastasis. Cancer Res 2004;64: 3737–40.
24. Krishnan J, Kirkin V, Steffen A, et al. Differential *in vivo* and *in vitro* expression of vascular endothelial growth factor (VEGF)-C and VEGF-D in tumors and its relationship to lymphatic metastasis in immunocompetent rats. Cancer Res 2003;63:713–22.
25. Kozaki K, Miyaishi O, Tsukamoto T, Tatematsu Y, Hida T, Takahashi T. Establishment and characterization of a human lung cancer cell line NCI-H460-LNM35 with consistent lymphogenous metastasis via both subcutaneous and orthotopic propagation. Cancer Res 2000;60:2535–40.
26. Paterna JC, Moccetti T, Mura A, Feldon J, Bueler H. Influence of promoter and WHV post-transcriptional regulatory element on AAV-mediated transgene expression in the rat brain. Gene Ther 2000;7: 1304–11.
27. Niwa H, Yamamura K, Miyazaki J. Efficient selection for high-expression transfectants with a novel eukaryotic vector. Gene 1991;108:193–9.
28. Laitinen M, Makinen K, Manninen H, et al. Adenovirus-mediated gene transfer to lower limb artery of patients with chronic critical leg ischemia. Hum Gene Ther 1998;9:1481–6.
29. Warri AM, Huovinen RL, Laine AM, Martikainen PM, Harkonen PL. Apoptosis in toremifene-induced growth inhibition of human breast cancer cells *in vivo* and *in vitro*. J Natl Cancer Inst 1993;85:1412–8.
30. Karkkainen MJ, Haiko P, Sainio K, et al. Vascular endothelial growth factor C is required for sprouting of the first lymphatic vessels from embryonic veins. Nat Immunol 2004;5:74–80.
31. Prevo R, Banerji S, Ferguson DJ, Clasper S, Jackson DG. Mouse LYVE-1 is an endocytic receptor for hyaluronan in lymphatic endothelium. J Biol Chem 2001;276:19420–30.
32. Sugino T, Kusakabe T, Hoshi N, et al. An invasion-independent pathway of blood-borne metastasis: a new murine mammary tumor model. Am J Pathol 2002;160: 1973–80.
33. Paavonen K, Puolakkainen P, Jussila L, Jahkola T, Alitalo K. Vascular endothelial growth factor receptor-3 in lymphangiogenesis in wound healing. Am J Pathol 2000;156:1499–504.
34. Mattfeldt T, Kestler HA, Sinn HP. Prediction of the axillary lymph node status in mammary cancer on the basis of clinicopathological data and flow cytometry. Med Biol Eng Comput 2004;42:733–9.